IL NUOVO CIMENTO **45 C** (2022) 85
DOI 10.1393/ncc/i2022-22085-8

COMMUNICATIONS: SIF Congress 2021

Characterization of a SiC detector for dosimetric application

M. GUARRERA([1])([2])(*) on behalf of G. PETRINGA([2])([3]), S. TUDISCO([2]) and G. A. P. CIRRONE([2])

([1]) *Department of Physics and Astronomy "Ettore Majorana", University of Catania - Catania, Italy*
([2]) *INFN, Laboratori Nazionali del Sud - Catania, Italy*
([3]) *ELI-Beamlines, Institute of Physics (FZU), Czech Academy of Sciences - Prague, Czechia*

received 26 March 2022

Summary. — New detectors development for dose monitoring in radiotherapy application is a very active field. Silicon carbide (SiC) devices are considered promising candidates, mainly due to their radiation hardness, wide bandgap, high electron saturation velocity, linearity with energy and independent response from dose rate. These properties make them suitable also for the detection of very high intensity particle beams, for which conventional semiconductor detectors cannot adequately perform. In this work a first *I-V* characterization of a 10 μm thick SiC detector embedded in epoxy resin before and after its immersion in water is discussed. The detecor's depletion voltage, capacitance, stability, linearity and reproducibility were evaluated as well. The results demonstrate that the potting technique and immersion in water do not affect the functionality of the detector, making it a good candidate for dosimetric applications.

1. – Introduction

Since the last two decades, the research in applied and biomedical physics devoted to the development of new detection systems dedicated to dosimetry has been very active. The effort in this field resulted in an emerging and increasing interest in Silicon Carbide (SiC) technology [1-30]. To perform accurate dosimetric measurements it is recommended to have detectors with tissue-equivalence characteristic, high spatial resolution and independent response from dose rate. It is also important to have fast response, high signal stability and linearity with energy in the widest possible dynamic range [31]. Diamond, silicon or silicon carbide devices have been investigated as possible candidates to satisfy the aforementioned requirements. In fact, semiconductor detectors suit many aspects of

(*) E-mail: guarrera@lns.infn.it

quality assurance programs and *in vivo* dosimetry [31]. Silicon diodes have been the primary devices used as *in vivo* dosimeters, thanks to their sensitivity to radiation at no-bias voltage, good stability and small size. However, silicon is not a tissue-equivalent material due to its high atomic number ($Z = 14$) compared to that of tissue ($Z_{eff} = 7.64$), which leads to a dosimetric response strongly dependent on radiation energy [3-5]. Silicon detectors have also some other disadvantages, such as dose rate dependence, angular dependence and radiation damage susceptibility [31]. This seriously restricts their operation in high radiation fields at room temperature [5-8]. On the other side, tests on diamond [9-15] and silicon carbide [1-3, 19-23] detectors exposed to particle irradiation strongly encourage the use of these devices in radiation dosimetry, also in severe radiation environments. Unluckily, diamond-based devices have the disadvantage of being very expensive as a consequence of the difficulty of selecting stones with the appropriate dosimetric properties [1]. An alternative with a potentially lower production cost is represented by chemical vapor deposition (CVD) diamond films [15-18]. On the other hand, their use in radiation dosimetry presents a limitation in both the charge collection efficiency and the uniformity of the electrical quality across the area. These limitations affect the sensitivity and the spatial resolution of the device [1, 2]. For these reasons the interests of the research community in this field turned towards the SiC detectors. SiC is one of the hardest materials found in nature, a condition which makes it very resistant to radiation damage. It exists in more than 200 different polytypes; among them, the 4H-SiC is nowadays considered the most appropriate for high-power, high-frequency and high-temperature applications [19]. Accordingly, 4H-SiC is particularly suitable for the detection of the next generation laser-driven particles beams, which are characterized by very intense short pulses of particles and able to release high dose in a very short time (dose rate up to 10^9 Gy/s) [22, 32-34].

Table I compares the main physical properties of silicon carbide (4H-SiC type), silicon and diamond detectors. SiC characteristics are interesting for developing radiation dosimeters, even if it is not nearly as tissue-equivalent ($Z_{eff} \simeq 10$) as diamond [3]. The most beneficial inherent material properties of 4H-SiC over Si listed in table I are its exceptionally high breakdown electric field, wide bandgap energy, high carrier saturation drift velocity, high displacement atom energy and high thermal conductivity [3, 25, 28, 33].

TABLE I. – *Principal properties at room temperature of 4H-SiC compared to silicon and diamond* [3, 25, 28, 35].

Property	4H-SiC	Si	Diamond
Bandgap energy (eV)	3.27	1.12	5.5
Hole mobility (cm^2/Vs)	115	460	1200
Electron mobility (cm^2/Vs)	800	1300	1800
Breakdown electric field (MV/cm)	3.0	0.3	10
Threshold displacement atom energy (eV)	22–35	13–20	40–50
Thermal conduct. (W/cmC)	3.0–5.0	1.5	20
Saturated electron velocity (cm/s 10^7)	2	1.0	2.2
Max working temperature (°C)	1240	300	1100
e-h pair energy (eV)	7.78	3.62	13
Density (g/cm^3)	3.22	2.33	3.52
Atomic number Z	10	14	6

The wide bandgap energy allows SiC to maintain semiconductor behavior, which in turn implies low leakage currents, at much higher temperature than silicon [28]. In addition, due to the high energy gap, SiC does not detect the visible radiation emitted from plasmas but it detects very well UV, X-rays, electrons and ions with a good level of signal-to-noise ratio at room temperature [22]. A small enough electron-hole pair generation energy is important to ensure a higher signal-to-noise ratio [28]. In this case, SiC performs better than diamond, while it is exceeded by Si. Another important aspect is the silicon-carbon displacement energy which makes SiC devices more resistant to radiation damage than Si ones and capable to operate for longer periods of time with unchanged detection properties [20-22]. The high critical breakdown field allows operation at high internal electric fields, minimizing the carrier transit time and the trapping probability. It makes also having low reverse current possible even at the very high electrical voltage. The high carrier saturation velocity, high electrons and holes mobilities imply high response velocity and a fast collection [22,24]. Moreover, the response of SiC devices is independent of the dose rate and linear with respect to the radiation energy released in the active region of the detector, whose depth depends on the doping concentration and reverse applied voltage [23, 24, 29-31, 33]. The high radiation hardness as well as the independence on dose rate make SiC a good candidate for FLASH Radiotherapy (FLASH-RT) applications, a novel methodology based on the use of ultra-high dose rate ($\geq 40\,\mathrm{Gy/\,s}$) beams [36-38].

In this work a new generation of solid-state device based on SiC technology was investigated for dosimetric applications. The detector was manufactured in the context of a collaboration between INFN (Italian Institute for Nuclear Physics) and IMM-CNR (Microelectronic and Microsystems Institute). It is a p-n junction device and it was built by using new technological processes developed in collaboration with ST-Microelectronics (STM) in Catania. It was also embedded in epoxy resin which makes the detector waterproof and immersible in water. Some other performances can be found in previous works [19, 27].

2. – Experimental setup and procedure

2˙1. *Detector description.* – The SiC device presented in this work has a $0.3\,\mu$m thick p-layer with a doping concentration $N_A = 10^{19}\,\mathrm{cm}^{-3}$ and a $10\,\mu$m thick n-layer with a doping concentration $N_D = 0.5\text{–}1\cdot10^{14}\,\mathrm{cm}^{-3}$. The detector has an active area of $1\cdot1\ \mathrm{cm}^2$ and is mounted on a PCB board (fig. 1(a)). An epoxy resin was used in order to make the detector waterproof. In particular, EPO-TEK ® 509FM-1 resin was adopted for the coating process. It is a bi-component, optically opaque epoxy resin designed for potting of semiconductors, PCB and system-level electronics [35]. An aluminum box of $2.5\cdot2.5\,\mathrm{cm}^2$ for the detector housing was also realized. In fig. 1(b) the SiC detector after the potting process is shown. The connection cable was coated with the same process.

2˙2. *Experimental procedure.* – The *I-V* (current *vs.* voltage) and *C-V* (capacitance *vs.* voltage) characteristics of the detector under investigation were measured. The *I-V* profile is useful to establish the leakage current of the detector and its breakdown voltage, while the *C-V* profile allows an estimation of the detector depletion voltage and saturation capacitance. The stability, reproducibility and linearity of the detector response were also analyzed. Among these tests, the *I-V* acquisition was repeated after the immersion of the detector in water.

The current generated by the detector was measured with a KEITHLEY K6517B electrometer which was also used as detector bias. The signal from the electrometer was read

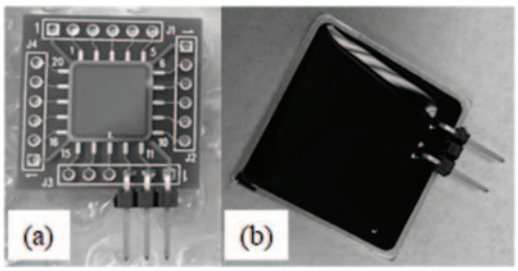

Fig. 1. – (a) The bare detector mounted on PCB. (b) The detector after the potting process.

connecting it to a personal computer via a serial interface. Data acquisition was made through two automatic housemade programs implemented in the LabView programming environment. A program routine was written to construct the *I-V* curve. This software allows the user to set several parameters such as sampling rate, input current range, voltage ramp and acquisition time. A program routine designed to construct both the *Q-t* (charge *vs.* time) and *I-t* (current *vs.* time) was also implemented accordingly. The *C-V* curve was measured by means of a HP precision LCR meter (model 4284A), while the bias voltage, once again supplied by the K6517B electrometer, was set manually. Detector irradiation was performed in vacuum using a source of Sr-90 (with a nominal activity of 33.3 MBq) housed in a plastic support designed to maintain both the position and the detector-source distance (fig. 2).

3. – Results

3˙1. *C-V characterization.* – The SiC capacitance C was measured at room temperature, in air and in the reverse bias voltage range of 0–100 V. The adopted capacimeter was set to operate at a full scale of 2 nF and with a sample rate of 1 kHz. Figure 3 shows the trend of $1/C^2$ as a function of applied bias. The curve obtained has a typical straight trend at low voltages (in the range 0–3 V), while it is almost constant at voltages higher than 50 V. A best-fit procedure was applied to find the linear functions that best approximate the two trends. The depletion voltage, obtained as the voltage value corresponding to the intersection of the two best-fit curves, was $V_D = 2.5 \pm 0.5$ V. The saturation capacity, determined as the minimum capacitance value obtained by increasing the reverse bias voltage, was $C_S = 860 \pm 5$ pF.

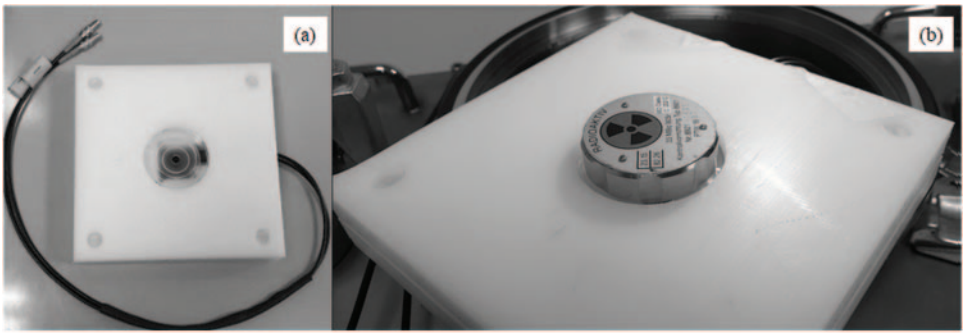

Fig. 2. – (a) The detector housed inside the holder. (b) Sr-90 source positioned on the support.

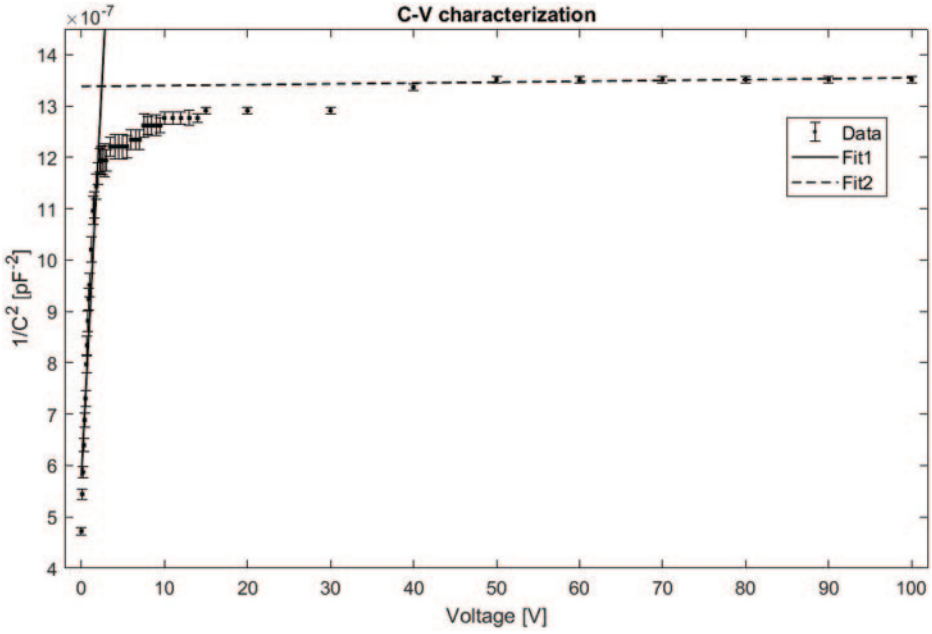

Fig. 3. – Trend of $1/C^2$ *vs.* reverse applied voltage. The capacitive contribution of the cables, estimated as 25 pF, was subtracted. The linear fits in the low voltage range (*Fit1*) and in the saturation region (*Fit2*) are also shown. Error bars are obtained by taking into account the reading error in the capacitance measurement.

Linearity, reproducibility and stability measurements were performed working at over depletion conditions corresponding to 50 V, in order to ensure a maximum drift velocity, necessary for a fast and complete charge collection.

3˙2. *Linearity and reproducibility measurements.* – Linearity and reproducibility tests of the detector response were performed by irradiating the detector in vacuum with the Sr-90 source. The detector was reversely polarized with 50 V and the charge was measured through the Q-t LabView program described in sect. **2˙2**. A full scale of 20 nC and four different acquisition times (5, 10, 15 and 20 s) were set. Eighty charge measurements for each acquisition time were acquired. Figure 4(a) shows the average charge values over time. The maximum percentage deviation was found to be 0.05%, indicating a high level of reproducibility of the charge response in these experimental conditions. A best-fit procedure was also performed to evaluate the linear trend, resulting in an R-square value very close to one. To better emphasize any deviation from the linear trend, the detector sensitivity was calculated. It is expressed as the ratio between the charge and the irradiation time (nC/ s) normalized to the expected value obtained through the fit curve. In fig. 4(b) the sensitivity as a function of the irradiation time is reported. Deviation from the linearity resulted to be within 0.03%.

3˙3. *Stability measurements.* – The detector stability was evaluated measuring the current response in the same experimental condition described in sect. **3˙2**. The current signal over time was acquired by means of the *I-t* Labview program. A full scale of 200 pA, an acquisition time of 20 s and a sample rate of 2 Hz

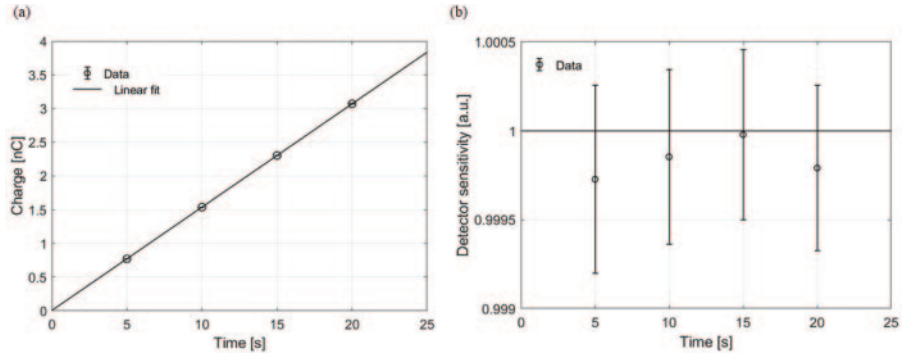

Fig. 4. – (a) Linearity of the absolute value of the detector charge response over time. Error bars are included in the points. (b) Deviation of the experimental points from the normalized linear trend. In both cases error bars represent the standard error of the mean.

were set. Five series of measurements were acquired, for a total acquisition time of 100 s and 200 values of current. The mean current value was -153 ± 2 pA, which corresponds to a relative error of 1.3%. We can conclude that the detector responds with a high degree of stability in these experimental conditions. Figure 5(b) shows the *I-V* curve of the detector under the irradiation of the Sr-90 source before its immersion in water (see sect. **3**˙4). In this case, the current obtained at 50 V is -156 ± 2 pA. The two current values are in agreement within the experimental errors.

3˙4. *I-V characterization.* – The *I-V* profile was investigated by applying a reverse bias voltage in the range between 0 and 100 V. Two different configurations —with and without the Sr-90 radioactive source— were adopted and the *I-V* Labview program described in sect. **2**˙2 was used in both cases. The acquisition was repeated three times for each voltage value setting a sampling rate of 2 Hz, a full scale of 200 pA and an acquisition time of 60 s. In fig. 5 the average trend of the different sets of measurements performed in both configurations is shown. Error bars are calculated by applying the error propagation theory and are respectively of the order of 2 pA and 0.5 pA for the configuration with and without the radioactive source.

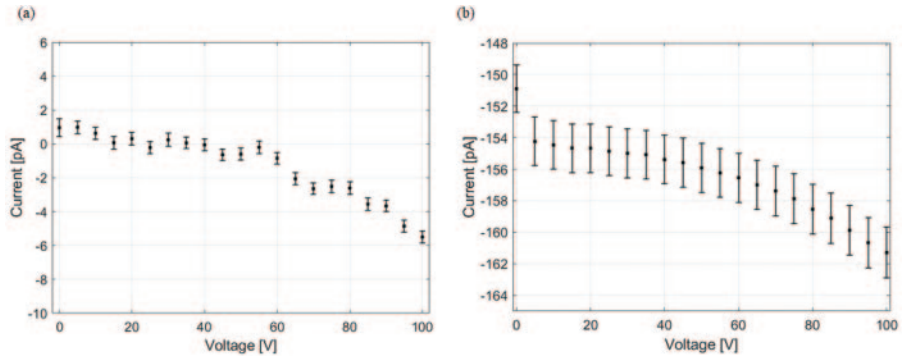

Fig. 5. – (a) Leakage current of the detector. (b) *I-V* detector profile with Sr-90 source. The current at 50 V is -156 ± 2 pA. In both cases the breakdown voltage is not reached.

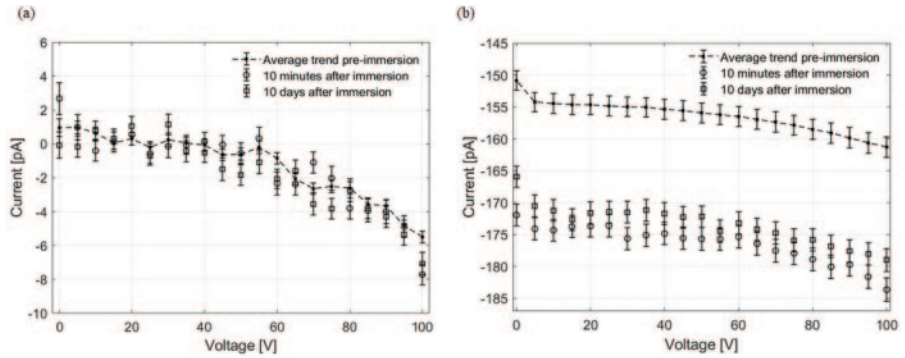

Fig. 6. – (a) Leakage current of the detector before and after immersion in water. No significant differences can be appreciated for most of the experimental points. (b) *I-V* profile with Sr-90 source before and after immersion in water. The current at 50 V reverse bias voltage 10 days after immersion is -172 ± 2 pA, which corresponds to a percentage deviation of the order of 10.5% with respect to the corresponding pre-immersion value. The absolute current values read 10 days after immersion in water are between 0.6% and 3.5% lower than those read 10 minutes after immersion.

Thereafter, the detector was immersed in water for one hour and both the *I-V* measurements were repeated under the same condition aforementioned. To establish the reproducibility level of the device response, the *I-V* acquisition was performed 10 minutes and 10 days after the immersion in water. In fig. 6 the comparison between all the measurements is shown. In order to quantify some possible effects due to the immersion in water, *i.e.*, detector contacts oxidation, the differences between pre and post immersion current were evaluated (see table II).

The comparison between the leakage currents acquired before and after the diving process exhibits an average difference of the order of 0.5 pA, while the maximum difference is 2.5 pA. Since most of the experimental data after immersion result to be within the error bars of the pre-immersion average trend, it is possible to conclude that no significant difference can be appreciated. The current produced by the detector under irradiation 10 minutes after immersion presents an average difference of the order of 20 pA as respect to the values measured before the immersion. The absolute current values read 10 days after immersion in water are on average 3 pA lower than those read 10 minutes after immersion, resulting within the experimental error.

TABLE II. – *Average difference between current signals acquired before (pre-imm.) and after immersion (post-imm.) in different configurations.*

	Configurations	Average differences
No external source	10 min. and 10 days post-imm. *vs.* pre-imm.	0.5 pA
With Sr-90 source	10 min. post-imm. *vs.* pre-imm.	20 pA
	10 min. post-imm. *vs.* 10 days post-imm.	3 pA

The obtained preliminary results indicate that the immersion may have somehow modified the resin properties, affecting the charge collection of the detector. Further investigations are needed to clarify the observed effect. However, it is possible to assert that the immersion did not damage the detector functionality.

4. – Conclusion

In this work a new generation of SiC detector based on p-n junction and embedded in epoxy resin was investigated for dosimetric applications. The detector was characterized to define its depletion voltage, capacitance and leakage current. Stability, reproducibility and linearity were also investigated. The results show good accordance with respect to previous works [19, 27], proving the detector's high level of performance even after the resin process. The depletion voltage remains at very low values, showing that the detector is a good candidate for *in vivo* dosimetry [3]. The comparison of I-V profiles before and after immersion in water was also performed. The leakage current, which is related to the intrinsic operational properties of the detector, did not show significant changes, while a mean difference of 11.3% was found in the current produced by the detector under irradiation after immersion. This suggests that the immersion may have somehow changed the characteristics of the resin. Further analysis is needed to better explain the observed effects. These preliminary results encourage to continue the investigation aimed at evaluating the potential use of the SiC detector coated with epoxy resin as a relative dosimeter immersed in water [39]. Future work will include dosimetric characterization tests with proton, electron and photon beams. The SiC performances will be compared with respect to the reference dosimeter already applied in clinical practice, *i.e.*, ionization chamber.

REFERENCES

[1] Bruzzi M. *et al.*, *Appl. Surf. Sci.*, **184** (2001) 245.
[2] Bruzzi M. *et al.*, *Diam. Relat. Mater.*, **10** (2001) 657.
[3] Bertuccio G. *et al.*, *IEEE Trans. Nucl. Sci.*, **61** (2014) 961.
[4] Jursinic P. A., *Med. Phys.*, **28** (2001) 1718.
[5] Bruzzi M. *et al.*, *Appl. Phys. Lett.*, **90** (2007) 172109.
[6] Borchi E. *et al.*, *IEEE Trans. Nucl. Sci.*, **45** (1998) 141.
[7] Nilsson B. *et al.*, *Radiother. Oncol.*, **11** (1988) 279.
[8] Bruzzi M., *IEEE Trans. Nucl. Sci.*, **90** (2001) 960.
[9] Meier D. *et al.*, *Nucl. Instrum. Methods A*, **426** (1999) 173.
[10] Burgemeister E. A., *Phys. Med. Biol.*, **26** (1981) 269.
[11] Cotty W. F., *Nature*, **177** (1956) 1075.
[12] Kozlov S. *et al.*, *Nucl. Instrum. Methods*, **117** (1974) 277.
[13] Planskoy B., *Phys. Med. Biol.*, **25** (1980) 519.
[14] Yoder M. N., *Nav. Res. Rev.*, **39** (1987) 27.
[15] Ciancaglioni I. *et al.*, *Med. Phys.*, **39** (2012) 4493.
[16] Bruzzi M. *et al.*, *Appl. Phys. Lett.*, **81** (2002) 298.
[17] Bruzzi M. *et al.*, *Nucl. Instrum. Methods A*, **454** (2000) 142.
[18] Bruzzi M. *et al.*, *IEEE Trans. Nucl. Sci.*, **47** (2000) 1430.
[19] Tudisco S. *et al.*, *Sensors*, **18** (2018) 2289.
[20] McLean F. B. *et al.*, *IEEE Trans. Nucl. Sci.*, **41** (1994) 1884.
[21] Sciortino S. *et al.*, *Nucl. Instrum. Methods A*, **552** (2005) 138.

[22] Cannavò A. *et al.*, in *Proceedings of 5th Workshop-Plasmi, Sorgenti, Biofisica ed Applicazioni, Department of Mathematics and Physics, University of Salento (Italy), 15–14 October 2016*, edited by Nassisi V. and Delle Side D., Vol. **2016** (ESE - Salento University Publishing) 2017, pp. 23–27.
[23] Bruzzi M. *et al.*, in *Proceedings of the International Symposium on Optical Science and Technology, San Diego (CA, United States), 30 July - 4 August 2000*, edited by James R. B. and Schirato R. C., *Hard X-Ray, Gamma-Ray, and Neutron Detector Physics II,* Vol. **4141** (SPIE) 2000, p. 48.
[24] De Napoli M. *et al.*, *Nucl. Instrum. Methods A*, **572** (2007) 831.
[25] Moscatelli F. *et al.*, *Mater. Sci. Forum*, **483-485** (2005) 1021.
[26] Ruddy F. H. *et al.*, *Nucl. Instrum. Methods A*, **505** (2003) 159.
[27] Petringa G. *et al.*, *JINST*, **15** (2020) C05023.
[28] Nava F. *et al.*, *Meas. Sci. Technol.*, **19** (2008) 102001.
[29] Bernat R. *et al.*, *Crystals*, **11** (2021) 1.
[30] Kada W. *et al.*, *J. Phys.: Conf. Ser.*, **1662** (2021) 1.
[31] Rozenfeld A. B., in *Proceedings of Concepts And Trends In Medical Radiation Dosimetry Conference, Wollongong (Australia), 15–18 September 2010*, edited by Rosenfeld A., Kron T., D'Errico F. and Moscovitch M., Vol. **1345** (American Institute of Physics) 2011.
[32] Macchi A. *et al.*, *Rev. Mod. Phys.*, **85** (2013) 751.
[33] Torrisi L. *et al.*, in *Proceedings of the 4th Workshop-Plasmi, Sorgenti, Biofisica ed Applicazioni, Lecce (Italy), 17-18 October 2014*, edited by Nassisi V., Delle Side D. and Giuffreda E., Vol. **2014** (ESE - Salento University Publishing) 2015, pp. 69–73.
[34] Torrisi L. *et al.*, in *Proceedings of the EUV and X-ray Optics: Synergy between Laboratory and Space VI (2019)*, edited by Hudec R. and Pina L., Vol. **11032** (SPIE) 2019.
[35] `https://www.epotek.com/docs/en/Datasheet/509FM-1.pdf`.
[36] De Kruijff R. M., *Int. J. Radiat. Biol.*, **96** (2020) 419.
[37] Esplen N. *et al.*, *Phys. Med. Biol.*, **65** (2020) 23TR03.
[38] Lin B. *et al.*, *Front. Oncol.*, **11** (2021) 644400.
[39] IAEA, Technical Reports Series No. 398, *Absorbed Dose Determination in External Beam Radiotherapy: An International Code of Practice for Dosimetry based on Standards of Absorbed Dose to Water* (IAEA, Vienna) 2000.